Laser Cooling in Semiconductor Heterojunctions by Extraction of Photogenerated Carriers

Paul Dalla Valle, Marc Bescond, Fabienne Michelini, Nicolas Cavassilas

Laser cooling in semiconductor heterojunctions by photogenerated carrier extraction

Paul Dalla Valle,[1] Marc Bescond,[1,2] Fabienne Michelini,[1] and Nicolas Cavassilas[1]

[1] *Aix Marseille Université, CNRS, Université de Toulon, IM2NP UMR 7334, 13397, Marseille, France*

[2] *Institute of Industrial Science, University of Tokyo, 4-6-1 Komaba, Meguro-ku Tokyo 153-8505, Japan*

Abstract

$\eta_{rad}\ \phi_{in}(E)$ Laser cooling of a semiconductor material, in which heat is extracted by emitting photons, requires a near-perfect external radiative efficiency. In this theoretical work, we propose a cooling system based on carrier extraction in a large gap reservoir. The electron-hole pairs generated in the material to be cooled are extracted in such a reservoir by absorbing phonons, then carrying a heat flux. With an analytical detailed balance model, we show that this concept is applicable even in materials with moderate external radiative efficiency. Moreover, by adjusting the gap of the reservoir to the laser power, this system can either reach high efficiency or transfer high power with lower efficiency.

I. INTRODUCTION

Optical refrigeration of solids, originally proposed in 1929, is based on anti-Stokes fluorescence, where the extracted photoluminescent energy exceeds the energy of the incident photons. This up-conversion process is induced by the absorption of thermal energy from the system, leading to its cooling [1]. Epstein et al. reported in 1995 the first experimental evidence of laser-induced refrigeration in a Yb^{3+}-doped glass [2]. Since then, many advances in the field of rare-earth-doped solids have been reported and reviewed [3, 4]. Besides, a high interest has grown for optical refrigeration of semiconductors to enhance the performance of many optoelectronic devices [5]. The refrigeration of semiconductor materials with a laser requires a laser energy very close to the bandgap energy or even lower [6]. Based on the Sheik-Bahae/Epstein theory [7], the net laser cooling of a semiconductor can occur in three different ways: possessing a large energy difference between the mean photoemission and the incident photons, having an external radiative efficiency (ERE) close to unity, and having an absorption efficiency near unity [8]. Laser cooling has been investigated in various semiconductors [3, 4]. In II-VI materials, Zhang et al. observed a cooling of 40 K in CdS nanobelts [8]. Ha et al. reported a net cooling directly from ambient temperature in lead halide perovskite thanks to a strong photoluminescence up-conversion and ERE of 99.8% [9]. A dominant anti-Stokes photoluminescent was reported in germanium nanocrystals, and a laser cooling of 50 K was inferred [5]. In III-V semiconductors, even if up-conversion processes have been highlighted, no net cooling was observed because of residual below gap absorption [10] or because ERE was not sufficient [11, 12]. Theoretical efforts were conducted to improve the optical refrigeration of semiconductors. Previous studies highlighted the importance of excitonic resonance [13] and photon recycling [14, 15]. Coupled quantum wells [16] and bandgap engineering [17] were proposed to improve the net cooling efficiency.

In this theoretical work, we propose to base the cooling on the extraction of the carriers into a larger bandgap reservoir, instead of their recombination. From a detailed-balance model, we show that extraction-based laser cooling can be much more efficient than the one obtained from radiative recombination. Interestingly, this method works even with modest ERE. For that, a type I heterojunction, consisting of a small-gap absorber connected to a large-gap reservoir, can transport thermal energy from the absorber to the reservoir in the form of potential carrier energy. The laser must photogenerate carriers in the absorber

with an energy lower than the bandgap energy of the reservoir. Those carriers are extracted into the reservoir by absorbing phonons, leading to evaporative cooling in the absorber. By adjusting the band offsets between the absorber and the reservoir, it will be possible to either have a high efficiency at low power or a higher power with a lower efficiency. We note that our proposal is very general and the concept of extraction-based optical refrigeration should apply to any type I heterojunction.

This article is organized as follows. We first describe the system and the approach used to model it. Then, by varying the system's architecture, we highlight the origin of the cooling process. Finally, with realistic parameters, we show that this process leads to high cooling power, even with modest ERE.

II. MODEL

For the sake of clarity, before the simple type I heterojunction, we consider a double heterojunction shown in Fig. 1. An semiconducting absorber, with a bandgap E_g, is set between two reservoirs. The left (right) reservoir creates a contact in the valence (conduction) band but offers an infinite barrier in the conduction (valence) band. When an electron-hole pair is generated in the absorber, apart from recombining, the electron (hole) can only go to the right (left) reservoir. This system then behaves like a solar cell [18]. We design the reservoirs in such a way that the energy difference between the valence band maximum of the left reservoir and the conduction band minimum of the right reservoir, called E_{cv}, is greater than E_g. An electron in the bottom of the conduction band of the absorber must absorb phonons to reach the right reservoir (same for holes and the left reservoir). In our model, the reservoirs are of infinite size. Thus, they can accept or provide as many carriers as necessary, without modifying their electronic distribution which remains at 300 K. Finally, the Fermi levels of these two reservoirs can be shifted by applying a bias $V = \mu_R - \mu_L$.

To model this system, we use a detailed-balance approach. In the absorber, we assume a generation rate of electron-hole pairs equal to the photon flux

$$\begin{cases} J_{gen} = \int_{E_g}^{\infty} \mathrm{LASER}(E)\mathrm{d}E \\ P_{gen} = \int_{E_g}^{\infty} \mathrm{LASER}(E) \cdot E\mathrm{d}E \end{cases} \tag{1}$$

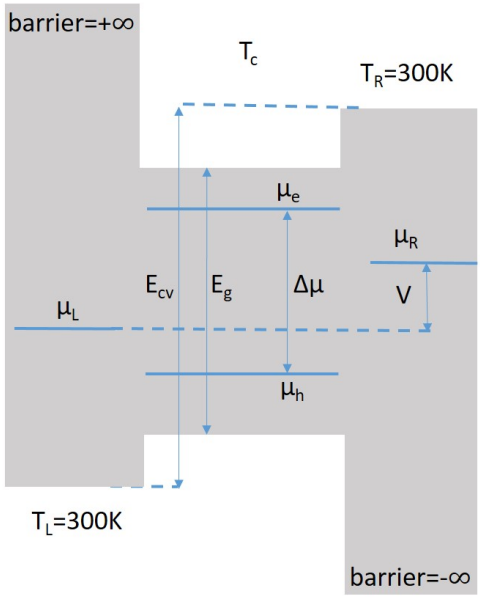

FIG. 1. Schematic representation of the double heterojunction. This system is made of a small gap absorber, between two reservoirs. In the whole system, the phonon temperature is set to 300 K. We do not model the cooling of the materials but only the heat fluxes. In the reservoirs, electrons are always considered at 300 K, and we apply a bias between the Fermi levels such that $V = \mu_R - \mu_L$. In our model, by solving the carriers and power fluxes conservation equations, we calculate T_c and $\Delta\mu = \mu_e - \mu_h$ for given E_g, E_{cv}, V and illumination.

where J_{gen} is the photon flux and P_{gen} the corresponding power flux density. In the following, we use a boxcar function to simulate the laser spectrum LASER(E).

Once generated, we assume that electrons and holes thermalize instantaneously via carrier-carrier interactions [19]. Their distribution is then a Fermi function with a temperature and a Fermi level that must be determined. We assume the same temperature T_c for electrons and holes, but different Fermi levels μ_e and μ_h with $\Delta\mu = \mu_e - \mu_h$. In our model, we consider that the crystal lattice remains at T_{amb}=300 K, meaning that the phononic bath remains at 300 K. Therefore, if T_c is different from 300 K, the carriers and the phonons are not at equilibrium with each other. It implies an exchange of energy in the direction of equilibrium. Obtaining $T_c > 300$ K means that the carriers emit phonons and thus, there is a heat transfer from the electronic bath toward the phononic bath. On the contrary, if $T_c < 300$ K, there is an absorption of phonons and thus a heat transfer in the reverse direction. Recent experimental results [20], concerning hot carriers solar cells, show

that the power exchanged with the phononic bath can be expressed as

$$P_{phonon}(T_c) = Q(T_c - T_{amb}) \tag{2}$$

where Q is a coefficient specific to each material and system (quantum well or bulk for example). The higher this parameter is, the more efficient the energy transfer between the electronic and phononic baths is. It offers a simple way to simulate the consequences of complex behaviours such as electron-optical phonon interactions, electron-acoustic phonon interactions and acoustic phonon-optical phonon interactions. For bulk GaAs, $Q = 2 \times 10^5$ W.m^{-2}.K^{-1} for a thickness of 100 nm (which is sufficient to absorb the photon flux). At first, we will use this value for our implementations. Subsequently, by varying Q over several orders of magnitude, we will show that this factor has very little importance on the cooling efficiency of our system. If $T_c < T_{amb}$, carriers in the absorber have consumed phonons, then P_{phonon} is negative.

Once generated and thermalized, the carriers can recombine. To simulate this recombination, we follow the approach given by Tsai[19]. If the conditions $E \gg k_B T$ and $(E - \Delta\mu) \gg k_B T$ are astisfied, we can express the electronic distribution using the Maxwell-Boltzmann approximation. Thus,

$$\begin{cases} J_{rec}(\Delta\mu, T_c) = \frac{1}{ERE} \int_{E_g}^{\infty} \phi_{BB}(E) e^{\frac{\eta_c(T_c)E}{k_B T_{amb}}} e^{\frac{(1-\eta_c(T_c))\Delta\mu}{k_B T_{amb}}} \mathrm{d}E \\ P_{rec}(\Delta\mu, T_c) = \frac{1}{ERE} \int_{E_g}^{\infty} E \cdot \phi_{BB}(E) e^{\frac{\eta_c(T_c)E}{k_B T_{amb}}} e^{\frac{(1-\eta_c(T_c))\Delta\mu}{k_B T_{amb}}} \mathrm{d}E \end{cases} \tag{3}$$

where

$$\phi_{BB}(E) = \frac{2\pi}{h^3 c^2} \times \frac{E^2}{exp\left(\frac{E}{k_B T_{amb}}\right) - 1} \tag{4}$$

is the black body radiation at room temperature T_{amb}, given by the Plank's law, and

$$\eta_c(T_c) = 1 - \frac{T_{amb}}{T_c} \tag{5}$$

is the Carnot's efficiency. J_{rec} is the number of electron-hole pairs that recombine per unit of time and surface, and P_{rec} is the corresponding power flux density. The integral part

J_{rec} corresponds to the emission of a black body ϕ_{BB} of temperature T_c [19]. We then have radiative recombination (emission of photons). To consider non-radiative recombination we divide these radiative recombination by ERE. In III-V materials and lead halide perovskites, when they are pure, ERE is close to 1[9, 11]. On the other hand in IV-IV materials with an indirect gap, ERE can be much lower and could reach values as low as 10^{-4}[21].

Rather than recombining, the carriers can also be extracted into the reservoirs. We have a flux of carriers through the left and right contacts. To conserve the total current, these fluxes must be equal. In our model, we describe the conduction and valence bands using the effective mass approximation. Following a three-dimensional (3D) description of the Landauer approach, the spectral carrier flux through the contacts is proportional to the difference between the Fermi Dirac functions in the absorber and the reservoirs. Using the 3D density-of-states in the reservoirs, and the effective mass approximation, the carrier flux through the contacts and the corresponding power flux density can be expressed as

$$\begin{cases} J_{contact}(\Delta\mu, T_c) = \int_{E_{cv}}^{\infty} \frac{8\pi m^*}{h^3}(E - E_{cv}) \left(\frac{1}{1+exp\left(\frac{(1-\eta_c(T_c))(E-\Delta\mu)}{2k_B T_{amb}}\right)} - \frac{1}{1+exp\left(\frac{E-V}{2k_B T_{amb}}\right)} \right) \mathrm{d}E \\ P_{contact}(\Delta\mu, T_c) = \int_{E_{cv}}^{\infty} \frac{8\pi m^*}{h^3}(E - E_{cv}) \left(\frac{1}{1+exp\left(\frac{(1-\eta_c(T_c))(E-\Delta\mu)}{2k_B T_{amb}}\right)} - \frac{1}{1+exp\left(\frac{E-V}{2k_B T_{amb}}\right)} \right) E\mathrm{d}E. \end{cases} \quad (6)$$

The derivation of these expressions is presented in Appendix. As $J_{contact}$ and $P_{contact}$ are proportional to m^*, we use the limiting (smallest) effective mass for the implementation.

Finally, to describe the carrier distribution in the absorber, we calculate T_c and $\Delta\mu$ using the conservation of particles and power fluxes for a given bias V and a given reservoir bandgap E_{cv}

$$\begin{cases} J_{gen} = J_{rec}(\Delta\mu, T_c) + J_{contact}(\Delta\mu, T_c) \\ P_{gen} = P_{rec}(\Delta\mu, T_c) + P_{contact}(\Delta\mu, T_c) + P_{phonon}(T_c). \end{cases} \quad (7)$$

III. RESULTS AND DISCUSSIONS

Figure 2 shows (a) the current $J_{contact}$ (b) T_c and (c) $\Delta\mu$ as a function of the bias V for $E_g = 0.74$ eV, $E_{cv} = Eg + 0.25$ eV, $m^* = 0.08 \cdot m_0$ (with m_0 the free electron mass) and an incident power $P_{gen} = 800$ W.cm^{-2}. The laser generates photons with an energy between E_g

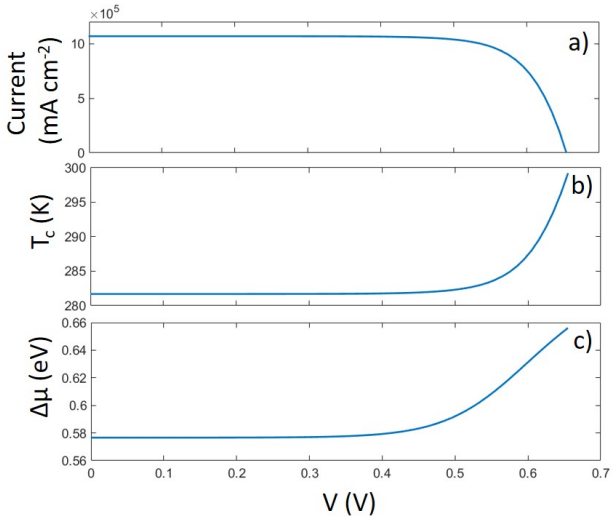

FIG. 2. (a) Charge current density $q \times J_{contact}$, (b) carrier temperature in the absorber T_c and (c) Fermi level splitting in the absorber $\Delta\mu$, as a function of the bias V applied between the two reservoirs. Calculations are conducted for $E_g = 0.47$ eV, $E_{cv} = 0.99$ eV, $ERE = 10^{-2}$, an illumination power of 800 W.cm^{-2} between E_g and $E_g + 10$ meV.

and $E_g + 10$ meV. This system offers the current-voltage characteristic of a solar cell with a short-circuit current density $J_{sc} = 1068$ A.cm^{-2} and an open-circuit voltage $V_{oc} = 0.655$ V. This is not surprising, since the system described in Fig. 1 is equivalent to a solar cell with the p (n) contact on the left (right). When $V = V_{oc}$, we have $T_c = 299$ K and $\Delta\mu = 0.656$ V. These values are respectively very close to the temperature of the reservoirs (300 K) and the voltage $V = 0.655$ V. The electrons (holes) in the absorber are almost in equilibrium with the electrons (holes) in the right (left) reservoir. At $V = 0$ V, $T_c = 282$ K and $\Delta\mu = 0.576$ V, much higher than V. We thus have an accumulation of cold carriers in the absorber which are no longer in equilibrium with the reservoirs.

To better understand the physical mechanism at $V = 0$ V, we show in Fig. 3 (a) T_c, and (b) $J_{contact}/J_{gen}$ and J_{rec}/J_{gen} for different values of $E_{cv} > E_g$ (with E_g constant). The laser power is fixed, meaning that J_{gen} and P_{gen} are constants. When $E_{cv} = E_g$, the carriers are easily extracted into the reservoirs ($J_{contact}/J_{gen} = 1$) and $T_c = 295$ K. On the other hand, when E_{cv} is large, the carriers are no longer extracted by the contacts ($J_{contact}/J_{gen} = 0$) and are all recombined ($J_{rec}/J_{gen} = 1$). We then find the behaviour of Fig. 2(b) at $V = V_{oc}$ (zero current and $T_c = 299$ K). Between these two extreme cases, T_c reaches a minimum. Starting

from $E_{cv} = E_g$, T_c decreases linearly with the increase of E_{cv}. Nevertheless, beyond a certain value of E_{cv}, the current $J_{contact}$ decreases and the temperature rises as J_{rec}/J_{gen}. The carrier temperature is thus the result of a trade-off between the energy at which the carriers are extracted and the extraction flux. We are therefore dealing with an evaporative cooling, i.e. when the extraction of high energy carriers cools the whole distribution [22]. This carrier cooling implies a thermal power flux from the phononic bath toward the electronic one, given by $-P_{phonon}$. Another way to interpret this process is that the carriers must absorb phonons to reach the contacts. The higher E_{cv} is, the more phonons are absorbed. Once the contact is reached, the carriers diffuse into the reservoir with this thermal energy as potential energy. If E_{cv} is too high, the carriers can no longer reach the contacts. In the case of Fig. 3, the best trade-off is obtained when $E_{cv} = E_g + 0.28$ eV.

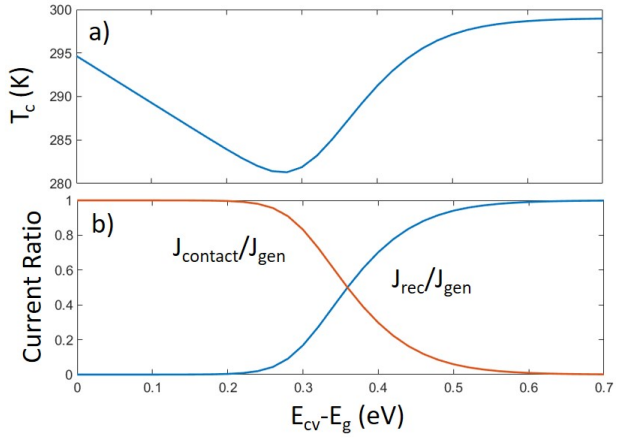

FIG. 3. For the same parameters than those used to obtain results shown in Fig. 2 (excepted E_{cv}), at $V = 0$ V, we represent (a) T_c and (b) the current ratios $J_{contact}/J_{gen}$ and J_{rec}/J_{gen} versus $E_{cv} - E_g$.

We now analyse the the carrier temperatures, presented in Fig. 3, with large E_{cv} and $E_{cv} = E_g$. When E_{cv} is large, the contacts isolate the absorber from the reservoirs and we are in the classical case of radiative cooling with a single material. The carriers have a temperature lower than 300 K (299 K) because they are photogenerated at an average energy (5 meV) lower than thermal energy. When $E_{cv} = E_g$, we obtain $T_c = 295$ K, the fact that this temperature is lower (295 K against 299 K) shows that the heat extraction through contacts is more efficient than the one based on recombination.

From the analysis performed on the solar cell, we now propose to design a cooling system

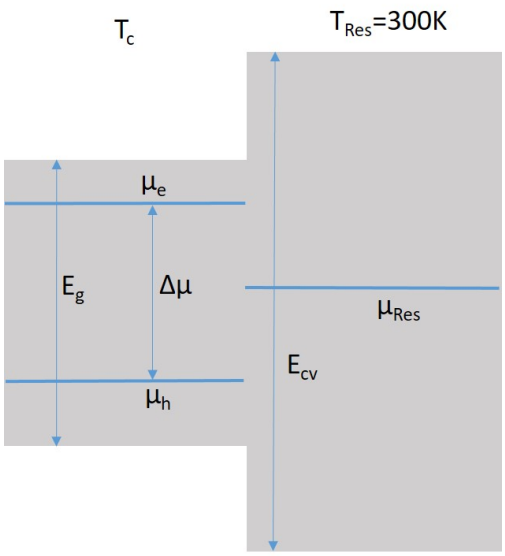

FIG. 4. Schematic representation of the system with one reservoir. The reservoir being infinite, all carriers injected from the absorber can recombine in the reservoir without Fermi level splitting between electrons and holes.

with a single reservoir, typically the type I heterojunction schematically shown in Fig. 4. Here, electrons and holes photogenerated in the absorber evaporate in the same reservoir. Such a reservoir has to be thick enough to allow the recombination of all the carriers injected from the absorber with a reduced Fermi level splitting. Considering an infinite reservoir in our model, all electrons and holes recombine while they share the same Fermi level μ_{Res} (equivalent to $V = 0$ V in the system presented in Fig. 1). We define the cooling efficiency as the ratio between the cooling power in the absorber and the generation power imposed by the laser. The cooling power is the balance between the phonons consumed through P_{phonon} and the phonons emitted through non-radiative recombiation in the absorber (i.e. $(1-ERE)\cdot P_{rec}$). As P_{phonon} is negative when phonons are extracted (see eq. 2), the cooling efficiency is defined as

$$\eta_{cooling} = \frac{-P_{phonon} - (1-ERE)\cdot P_{rec}}{P_{gen}}. \tag{8}$$

The efficiency $\eta_{cooling}$ is positive (cooling of the absorber) if P_{phonon} is negative, with an absolute value greater than $(1-ERE)\cdot P_{rec}$.

We explore the potentialities of an InGaAs/InP heterojunction as a cooling system con-

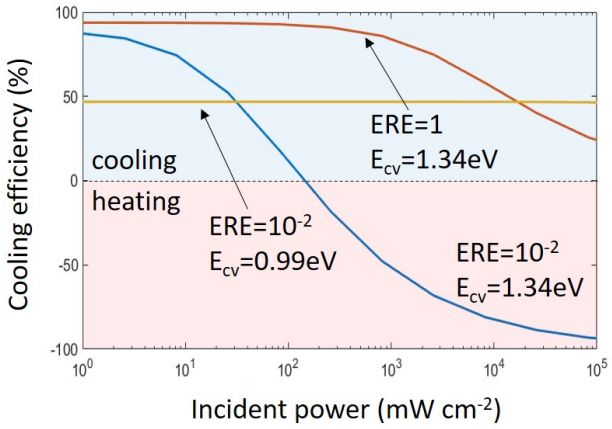

FIG. 5. Cooling efficiency $\eta_{cooling}$ versus the incident laser power considering a InGaAs/InP type I heterojunction as shown in Fig. 4 ($E_g = 0.74$ eV and $E_{cv} = 1.34$ eV) with $ERE = 1$ and 10^{-2}, and for a hypothetical case where E_{cv} is reduced to 0.99 eV.

trolled by a laser. We focus on this type I heterojunction to give a concrete example, but there is no evidence that this heterojunction is better than any other one for refrigeration. Considering InGaAs for the absorber ($E_g = 0.74$ eV) and InP for the infinite reservoir ($E_{cv} = 1.34$ eV), we compute the cooling efficiency versus the laser power P_{gen}, shown Fig. 5. We do this calculation for $ERE = 1$ and 10^{-2}. At low power, for both ERE, the process offers high efficiencies. With $ERE = 1(10^{-2})$, we obtain for instance an efficiency of 94% (82%) for $P_{gen} = 80$ mW.cm^{-2}, which gives a thermal power extracted from the absorber of 75 mW.cm^{-2} (66 mW.cm^{-2}). For higher laser powers, when $ERE = 1$, the cooling efficiency decreases but remains positive. In this ideal case, there is no source of heating since there is no non-radiative recombination. However, the efficiency decreases with the power P_{gen} because the contacts are not sufficient to extract all the photogenerated carriers. There is then a significative accumulation of carriers which implies strong radiative recombinations. We then approach a system with a single material, less efficient, where the extraction of power is done by radiative recombinations. With $ERE = 10^{-2}$, the efficiency decreases as P_{gen} increases and becomes negative, corresponding to the heating of the absorber. In this case, the accumulation of carriers implies non-radiative recombinations and therefore heating. For example, for $P_{gen} = 10^5$ mW.cm^{-2}, the efficiency drops to -93%. In order to reduce the accumulation of carriers and therefore recombinations, it would be necessary to choose a system offering a lower E_{cv}. With the same power P_{gen} and the same absorber

InGaAs and $ERE = 10^{-2}$, but with a reservoir such that $E_{cv} = 0.99$ eV (case of Fig. 2), we obtain an efficiency of 47%. As can be seen in Fig. 5, with this value of E_{cv}, the efficiency is very stable over the considered power range. We are therefore less efficient at low power, but more efficient at high power.

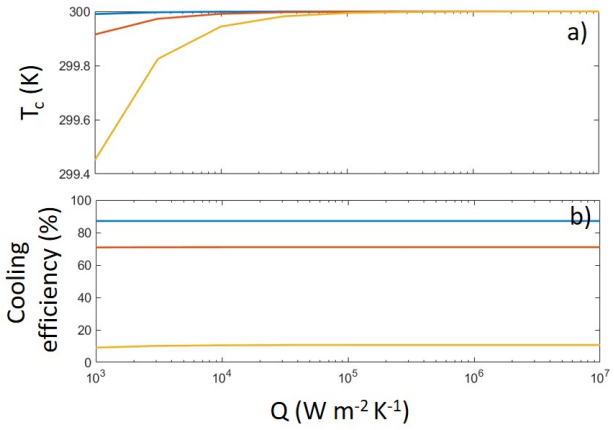

FIG. 6. (a) Carrier temperature T_c and (b) cooling efficiency $\eta_{cooling}$ versus the electron-phonon scattering parameter Q for incident laser power of (blue) 1 mW.cm^{-2}, (red) 10 mW.cm^{-2} and (yellow) 100 mW.cm^{-2}.

Here, we study the influence of the Q factor on our proposal. This parameter is related to the electron-phonon scattering in the material. The empirical law, given by Eq. 2, states that the power flux exchanged between the electronic and the phononic baths (P_{phonon}) is proportional to the temperature difference between these two baths ($T_c - T_{amb}$). This law comes from studies of hot-carrier solar cells based on III-V materials, but no value for other materials has yet been published. To establish the impact of Q on the operation of our device, we calculate the carrier temperature and the cooling efficiency over a wide range of Q (four orders of magnitude). We conduct these calculations for the InGaAs/InP heterostructure ($E_g = 0.74$ eV and $E_{cv} = 1.34$ eV) and $ERE = 10^{-2}$. As shown in Fig. 5, for such a device, the laser power (P_{gen}) must be smaller than 200 mW.cm^{-2} to induce a net cooling. We then consider three different laser powers: 1, 10 and 100 mW.cm^{-2}. Fig. 6(a) shows the variation of T_c versus Q. Although T_c varies with Q, for the considered range of Q and for the three laser powers, we have $\Delta T = T_c - T_{amb} < 0.6$ K. Fig. 6(b) shows the corresponding cooling efficiency $\eta_{cooling}$ versus Q for the same laser powers. Interestingly, the efficiency does not depend on Q. Indeed, for small ΔT, the Carnot's efficiency η_c tends

to 0 (Eq. 5) and consequently both P_{rec} and $P_{contact}$ are almost independent of T_c (Eq. 3 and Eq. 6, respectively). Therefore, P_{phonon} (Eq. 7) and the efficiency $\eta_{cooling}$ (Eq. 8) are both principally ruled by ERE, E_{cv}, E_g and the laser power. This last result is important because it shows that our proposal, operating at small ΔT, is very robust and can work with a large variety of materials. Its ability to cool efficiently is governed by the design of the heterojunction, the laser power and ERE. The electron-phonon scattering rate, even though affecting the carrier temperature, does not influence the cooling power.

Finally, to experimentally demonstrate the cooling behaviour of our device, we propose an optical characterisation showing the energy up-conversion of the carriers (absorption at E_g and emission at E_{cv}). An integrating sphere, recovering all the emitted photons, would enable us to measure the balance of the particle fluxes and the corresponding powers [23]. By measuring P_{gen}, P_{rec} and the power emitted by the reservoir and knowing the ERE of the absorber and the reservoir, one could deduce P_{phonon}. This characterisation will be dedicated to a future study.

IV. CONCLUSION

Using a detailed-balance model, we present an original cooling process in an absorber under radiation. The corresponding heat is transformed into carrier energy which is extracted into a large bandgap reservoir. A large gap difference between the reservoir and the absorber increases the energy carried by each carrier but reduces the number of these carriers. The best trade-off, which will guide the choice of materials, depends on the desired cooling power. Compared to cooling with a single material which requires an ERE close to 1, our proposal works even with a low ERE. Indeed, extracting heat via carrier transport rather than radiative recombination makes our system more efficient and adaptable to operating circumstances. Experimental confirmation of this process would be a major advance in heat management in semiconductor devices.

ACKNOWLEDGEMENT

The authors thank GELATO ANR project for financial support (ANR-21-CE50-0017).

---

[1] Peter Pringsheim, "Zwei Bemerkungen über den Unterschied von Lumineszenz- und Temperaturstrahlung," Zeitschrift für Physik **57**, 739–746 (1929).

[2] Richard I. Epstein, Melvin I. Buchwald, Bradley C. Edwards, Timothy R. Gosnell, and Carl E. Mungan, "Observation of laser-induced fluorescent cooling of a solid," Nature **377**, 500–503 (1995).

[3] Jyothis Thomas, Lauro Maia, Yannick Ledemi, Younes Messaddeq, and Raman Kashyap, "Emerging Trends, Challenges, and Applications in Solid-State Laser Cooling," in *Oxide Electronics* (John Wiley & Sons, Ltd, 2021) Chap. 10, pp. 353–396.

[4] Denis V. Seletskiy, Richard Epstein, and Mansoor Sheik-Bahae, "Laser cooling in solids: Advances and prospects," Reports on Progress in Physics **79**, 096401 (2016).

[5] Manuchehr Ebrahimi, Amr S. Helmy, and Nazir P. Kherani, "Plasmon Coupling—The Root Cause of Raman Anomaly and Laser Cooling in Nanocrystal Ge," Advanced Photonics Research **4**, 2200251 (2023).

[6] Muchuan Hua and Ricardo S. Decca, "Net energy up-conversion processes in CdSe/CdS (core/shell) quantum dots: A possible pathway towards optical cooling," Physical Review B **106**, 085421 (2022).

[7] Mansoor Sheik-Bahae and Richard I. Epstein, "Can Laser Light Cool Semiconductors?" Physical Review Letters **92**, 247403 (2004).

[8] Jun Zhang, Dehui Li, Renjie Chen, and Qihua Xiong, "Laser cooling of a semiconductor by 40 kelvin," Nature **493**, 504–508 (2013).

[9] Son-Tung Ha, Chao Shen, Jun Zhang, and Qihua Xiong, "Laser cooling of organic–inorganic lead halide perovskites," Nature Photonics **10**, 115–121 (2016).

[10] Daniel A. Bender, Jeffrey G. Cederberg, Chengao Wang, and Mansoor Sheik-Bahae, "Development of high quantum efficiency GaAs/GaInP double heterostructures for laser cooling," Applied Physics Letters **102**, 252102 (2013).

[11] H. Gauck, T. H. Gfroerer, M. J. Renn, E. A. Cornell, and K. A. Bertness, "External radiative quantum efficiency of 96% from a GaAs / GaInP heterostructure," Applied Physics A **64**, 143–147 (1997).

[12] Guan Sun, Ruolin Chen, Yujie J. Ding, and Jacob B. Khurgin, "Upconversion Due to Optical-Phonon-Assisted Anti-Stokes Photoluminescence in Bulk GaN," ACS Photonics **2**, 628–632 (2015).

[13] G. Rupper, N. H. Kwong, and R. Binder, "Large Excitonic Enhancement of Optical Refrigeration in Semiconductors," Physical Review Letters **97**, 117401 (2006).

[14] Kuan-Chen Lee and Shun-Tung Yen, "Photon recycling effect on electroluminescent refrigeration," Journal of Applied Physics **111**, 014511 (2012).

[15] J.-B. Wang, S. R. Johnson, D. Ding, S.-Q. Yu, and Y.-H. Zhang, "Influence of photon recycling on semiconductor luminescence refrigeration," Journal of Applied Physics **100**, 043502 (2006).

[16] Raphaël S. Daveau, Petru Tighineanu, Peter Lodahl, and Søren Stobbe, "Optical refrigeration with coupled quantum wells," Optics Express **23**, 25340–25349 (2015).

[17] Jacob B. Khurgin, "Band gap engineering for laser cooling of semiconductors," Journal of Applied Physics **100**, 113116 (2006).

[18] Nicolas Cavassilas, Imam Makhfudz, Anne-Marie Daré, Michel Lannoo, Guillaume Dangoisse, Marc Bescond, and Fabienne Michelini, "Theoretical Demonstration of Hot-Carrier Operation in an Ultrathin Solar Cell," Physical Review Applied **17**, 064001 (2022).

[19] Chin-Yi Tsai, "Theoretical model and simulation of carrier heating with effects of nonequilibrium hot phonons in semiconductor photovoltaic devices," Progress in Photovoltaics: Research and Applications **26**, 808–824 (2018).

[20] Maxime Giteau, Edouard de Moustier, Daniel Suchet, Hamidreza Esmaielpour, Hassanet Sodabanlu, Kentaroh Watanabe, Stéphane Collin, Jean-François Guillemoles, and Yoshitaka Okada, "Identification of surface and volume hot-carrier thermalization mechanisms in ultrathin GaAs layers," Journal of Applied Physics **128**, 193102 (2020).

[21] Martin A. Green, "Radiative efficiency of state-of-the-art photovoltaic cells: Radiative efficiency of photovoltaic cells," Progress in Photovoltaics: Research and Applications **20**, 472–476 (2012).

[22] Marc Bescond, Guillaume Dangoisse, Xiangyu Zhu, Chloé Salhani, and Kazuhiko Hirakawa, "Comprehensive Analysis of Electron Evaporative Cooling in Double-Barrier Semiconductor

Heterostructures," Physical Review Applied **17**, 014001 (2022).

[23] Kazunobu Kojima, Tomomi Ohtomo, Ken-ichiro Ikemura, Yoshiki Yamazaki, Makoto Saito, Hirotaka Ikeda, Kenji Fujito, and Shigefusa F. Chichibu, "Determination of absolute value of quantum efficiency of radiation in high quality GaN single crystals using an integrating sphere," Journal of Applied Physics **120**, 015704 (2016).

V. APPENDIX - DERIVATION OF $J_{contact}$ AND $P_{contact}$

In this appendix, we demonstrate the formulation of the carrier flux extracted from the left reservoir to the right reservoir ($J_{contact}$), and the corresponding power flux density ($P_{contact}$), in the system presented Fig. 1. These relations are given by Eq. 6. To derive this expression, we first consider a system with selective contacts, as presented Fig. 7.

We define J_{left} as the current flowing from the left reservoir to the absorber and J_{right} as the current flowing from the absorber to the right reservoir. These two currents are respectively depicted with red and blue arrows in Fig. 7. The current conservation implies that these two currents are equal, thus

$$J_{contact} = J_{left} = J_{right}. \tag{9}$$

To express J_{left} and J_{right} we use a three-dimensional (3D) description of the Landauer approach. Through selective contact with an energy window $\mathrm{d}E$, J_{right} is proportional to the difference between the electronic Fermi-Dirac distributions in the absorber and in the right reservoir. Thus,

$$J_{right} = 2 \cdot \frac{\rho_{3D_R}}{V} \cdot v_g \cdot (f_{abs_e} - f_{res_R}) \cdot \mathrm{d}E \tag{10}$$

where ρ_{3D_R} is the 3D density of state in the right reservoir, V is the volume and v_g is the group velocity of the carriers. Factor 2 accounts for spin degeneracy. f_{abs_e} and f_{res_R} are the Fermi-Dirac distributions of electrons in the absorber and in the right reservoir respectively. So,

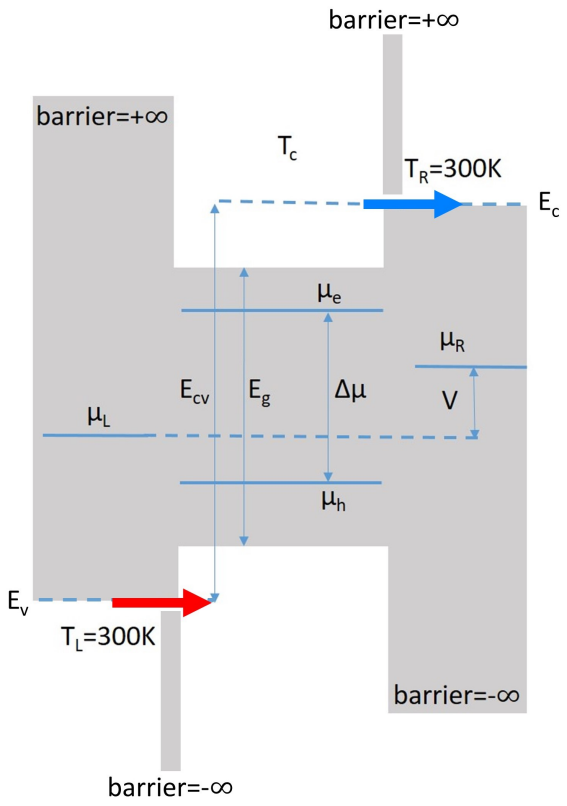

FIG. 7. Schematic representation of the double heterojunction device with selective contacts. Electrons are injected from the right contact to the absorber with energy $E = E_v$ (red arrow) and are extracted from the absorber to the right contact with energy $E = E_c$ (blue arrow). The notations are identical to Fig. 1

$$f_{abs_e} = \frac{1}{1 + exp\left(\frac{E_c - \mu_e}{k_B T_c}\right)} \tag{11}$$

and

$$f_{res_R} = \frac{1}{1 + exp\left(\frac{E_c - \mu_R}{k_B T_{amb}}\right)} \tag{12}$$

where E_c is the right contact selective energy, μ_e and μ_R are the electron pseudo-Fermi levels in the absorber and in the right reservoir respectively, k_B is the Boltzmann's constant and T_c and T_{amb} are the temperature in the absorber and in the right reservoir respectively.

Similarly, J_{left} is the electron current from the left contact to the absorber. For further simplifications, we express J_{left} as the hole current from the absorber to the left contact,

$$J_{left} = 2 \cdot \frac{\rho_{3D_L}}{V} \cdot v_g \cdot (f_{abs_h} - f_{res_L}) \times \mathrm{d}E \tag{13}$$

where ρ_{3D_L} is the 3D density of state in the left reservoir, f_{abs_h} and f_{res_L} are the Fermi-Dirac distributions of holes in the absorber and the left reservoir respectively,

$$f_{abs_h} = \frac{1}{1 + exp\left(\frac{\mu_h - E_v}{k_B T_c}\right)} \tag{14}$$

and

$$f_{res_L} = \frac{1}{1 + exp\left(\frac{\mu_L - E_v}{k_B T_{amb}}\right)} \tag{15}$$

where E_v is the left contact selective energy, μ_h and μ_L are the hole pseudo-Fermi levels in the absorber and in the left reservoir respectively. The 3D density of states in the left and right reservoirs is,

$$\rho_{3D_{L/R}} \cdot \mathrm{d}E = \frac{4\pi k_{L/R}^2 . \mathrm{d}k}{\frac{8\pi^3}{V}} \tag{16}$$

where $k_{L/R}$ is the 3D wave vector modulus in the left/right reservoir. We describe the kinetic energy of the carriers in the conduction and valence bands using the effective mass approximation, so

$$E_{k_{L/R}} = \frac{\hbar^2 k_{L/R}^2}{2m_{v/c}^*} \tag{17}$$

where $E_{k_{L/R}}$ is the kinetic energy in the left/right reservoir, $\hbar$ is the reduced Planck's constant and $m_{v/c}^*$ is the valence/conduction effective mass in the left/right reservoir. The group velocity v_g is

$$v_g = \frac{1}{\hbar} \cdot \frac{\mathrm{d}E}{\mathrm{d}k}. \tag{18}$$

We thus have,

$$J_{right} = 2 \cdot \frac{1}{V} \cdot \frac{V}{2\pi^2} \cdot k_R^2 \cdot \frac{\mathrm{d}k}{\mathrm{d}E} \cdot \frac{1}{\hbar} \cdot \frac{\mathrm{d}E}{\mathrm{d}k} \cdot (f_{abs_e} - f_{res_R}) \cdot \mathrm{d}E \tag{19}$$

$$J_{right} = \frac{2m_c^* E_{k_R}}{\pi^2 \hbar^3} \cdot (f_{abs_e} - f_{res_R}) \cdot \mathrm{d}E \tag{20}$$

$$J_{right} = \frac{16\pi m_c^*}{h^3} \cdot E_{k_R} \cdot (f_{abs_e} - f_{res_R}) \cdot \mathrm{d}E \tag{21}$$

and

$$J_{left} = \frac{16\pi m_v^*}{h^3} \cdot E_{k_L} \cdot (f_{abs_h} - f_{res_L}) \cdot \mathrm{d}E. \tag{22}$$

As $J_{contact} = J_{left} = J_{right}$, we have two distinct expressions for $J_{contact}$,

$$J_{contact} = \frac{16\pi m_c^*}{h^3} \cdot E_{k_R} \cdot \left(\frac{1}{1 + exp\left(\frac{E_c - \mu_e}{k_B T_c}\right)} - \frac{1}{1 + exp\left(\frac{E_c - \mu_R}{k_B T_{amb}}\right)} \right) \cdot \mathrm{d}E \tag{23}$$

$$J_{contact} = \frac{16\pi m_v^*}{h^3} \cdot E_{k_L} \cdot \left(\frac{1}{1 + exp\left(\frac{\mu_h - E_v}{k_B T_c}\right)} - \frac{1}{1 + exp\left(\frac{\mu_L - E_v}{k_B T_{amb}}\right)} \cdot \right) \cdot \mathrm{d}E. \tag{24}$$

We introduce the notation shown Fig. 7: $\Delta\mu = \mu_e - \mu_h$, $V = \mu_R - \mu_L$ and $E_{cv} = E_c - E_v$. The kinetic energy can be expressed as $E_{k_{L/R}} = \frac{E - E_{cv}}{2}$. We note that $J_{contact}$ is proportional to the effective mass, so we consider the limiting (smallest) one to go further: $m^* = \min\{m_c^*, m_v^*\}$, thus,

$$J_{contact} = \frac{16\pi m^*}{h^3} \cdot \frac{(E - E_{cv})}{2} \cdot \left(\frac{1}{1 + exp\left(\frac{E_c - \mu_e}{k_B T_c}\right)} - \frac{1}{1 + exp\left(\frac{E_c - \mu_R}{k_B T_{amb}}\right)} \right) \cdot \mathrm{d}E \tag{25}$$

$$J_{contact} = \frac{16\pi m^*}{h^3} \cdot \frac{(E - E_{cv})}{2} \cdot \left(\frac{1}{1 + exp\left(\frac{\mu_h - E_v}{k_B T_c}\right)} - \frac{1}{1 + exp\left(\frac{\mu_L - E_v}{k_B T_{amb}}\right)} \right) \cdot \mathrm{d}E \tag{26}$$

which requires that

$$\frac{E_c - \mu_e}{k_B T_c} = \frac{\mu_h - E_v}{k_B T_c} \tag{27}$$

and

$$\frac{E_c - \mu_R}{k_B T_{amb}} = \frac{\mu_L - E_v}{k_B T_{amb}} \tag{28}$$

leading to

$$J_{contact} = \frac{8\pi m^*}{h^3} \cdot (E - E_{cv}) \cdot \left(\frac{1}{1 + exp\left(\frac{E_{cv} - \Delta\mu}{2k_B T_c}\right)} - \frac{1}{1 + exp\left(\frac{E_{cv} - V}{2k_B T_{amb}}\right)} \right) \cdot \mathrm{d}E. \tag{29}$$

We note that with ideal selective contacts ($\mathrm{d}E \to 0$, and $E = E_{cv}$) $J_{contacts}$ tends to zero. To consider the system shown Fig. 1 (with semi-selective contacts) we integrate Eq. 29 from E_{cv} to ∞, thus

$$J_{contact} = \int_{E_{cv}}^{\infty} \frac{8\pi m^*}{h^3} \cdot (E - E_{cv}) \cdot \left(\frac{1}{1 + exp\left(\frac{E - \Delta\mu}{2k_B T_c}\right)} - \frac{1}{1 + exp\left(\frac{E - V}{2k_B T_{amb}}\right)} \right) \cdot \mathrm{d}E. \tag{30}$$

The carrier temperature in the absorber T_c can be expressed with the Carnot's efficiency (Eq. 5) as $T_c = \frac{T_{amb}}{(1-\eta_c)}$, leading to the expression d(Eq. 6). To derive the expression of $P_{contact}$, the corresponding power flux density, we simply note that with selective contacts, $P = J \cdot E$. After integration, we get the expression used in the main text.